ELSEVIER

Journal of Nuclear Materials 266–269 (1999) 1219–1223

journal of nuclear materials

Particle control and behaviour of neutrals in the pumped W-shaped divertor of JT-60U

H. Tamai *, N. Asakura, N. Hosogane, H. Takenaga, S. Higashijima, K. Itami, S. Konoshima, H. Kubo, A. Sakasai, S. Sakurai, K. Shimizu

Naka Fusion Research Establishment, Japan Atomic Energy Research Institute, Naka-machi, Ibaraki-ken, 311-0913 Japan

Abstract

As a trial for an active particle control, simultaneous feedback control of the divertor neutral pressure and main plasma density by the dual locations of gas puff is performed in the W-shaped divertor of JT-60U. At a relatively low gas-puffing rate, the divertor neutral pressure and main density are well controlled as pre-programmed. Lowering the X-point height is effective for isolation of the main plasma from divertor neutral particles. Simultaneous control has some difficulty at a high gas-puffing rate due to an increase of the cross-term coupling with each gas puff. Particle flux from the neutral beam also makes it difficult to control divertor neutral pressure and density. The simultaneous controllability depends on the operational region of the divertor neutral pressure and the main density. The coupling of the divertor neutral pressure with gas puff becomes larger in the high flux region, so that core fuelling in order to minimise the coupling is necessary for an effective particle isolation.

Keywords: Density control; Fuelling; JT-60U; Particle control; Pumped divertor

1. Introduction

Since high performance in the core plasma should be simultaneously realised with dense and cold divertor plasma, particle control to maintain a high divertor neutral pressure and low core fuelling is one of the key issues for the ITER task of divertor physics [1]. From this view point, experimental and theoretical studies on divertor physics have been initiated in various tokamak machines [2–4]. The pumped W-shaped divertor in JT-60U, which simulates the vertical target of ITER divertor design, is implemented to investigates the advantage of the divertor geometry and to construct the various databases for ITER design. The most attractive feature of the W-shaped divertors has been expected to realise the dense and cold divertor plasma with a reduced neutral back flow to the main plasma [5].

Reservoir effect for neutral particles in the baffle structure, strong asymmetry of the particle recycling between inside and outside divertor and the impurity suppression as the effect of the private dome are observed [6,7]. The divertor pumping also effectively prevents disruptions caused by the high recycling of neutral flux.

In such a W-shaped divertor, the isolation of the main plasma from divertor neutral particles is suggested as an effect of closure of the divertor private region. It is important to assess the shielding characteristic of neutral particles between the divertor and main plasma, and also to estimate the controllability of particle fuelling by gas puffing in the W-shaped divertor aimed for ITER design. As a trial for the active particle control, simultaneous feedback control of the divertor neutral pressure and the main plasma density is performed in the W-shaped divertor of JT-60U.

This paper reports the feasibility of the active particle control and estimates the coupling between the main and divertor region.

2. Diagnostic for divertor neutral pressure

During the modification to the W-shaped divertor, fast-response ionisation gauges were installed to in-

* Corresponding author. Tel.: +81 29 270 7341; fax: +81 29 270 7419; e-mail: tamai@naka.jaeri.go.jp

PII: S 0 0 2 2 - 3 1 1 5 (9 8) 0 0 6 8 7 - 4

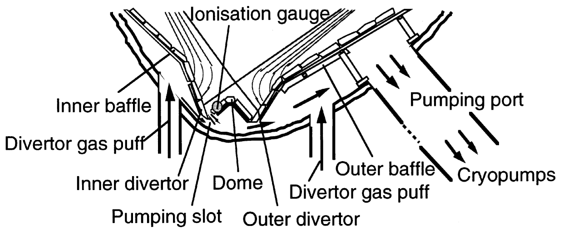

Fig. 1. Structure of W-shaped divertor, the fast-response ionisation gauge at the inside divertor and the location of divertor gas puff. Arrows indicate the gas flow under the dome and baffles.

vestigate the divertor neutral pressure. The gauge and its controller were developed by the ASDEX team [8,9]. The gauge head can be applied in strong magnetic fields, so that it can be located very close to the plasma, which ensures the fast time response.

In front of the gauge head a chevron is located in order to avoid the plasma exposure and to provide thermalisation of particles. The time response including the effect of the chevron is estimated to be about 3–4 ms, which is two orders of magnitude faster than conventional pressure gauges used in the vacuum vessel of JT-60U.

Feedback control of divertor neutral pressure, described below, is performed using the fast-response ionisation gauge at the inside divertor. Fig. 1 illustrates the structure of the W-shaped divertor, the fast-response ionisation gauge at the inside divertor and the location of divertor gas puff.

3. Feedback control of divertor neutral pressure

Since the intense gas puff is made to the divertor to achieve a dense and cold divertor plasma, the back flow of the divertor neutral into the main chamber should be suppressed to sustain the high performance of core plasma [10]. In addition, excessive gas puff into the divertor should also be avoided for the stability of the divertor plasma. In order to adjust the proper divertor gas puff, a feedback system has been implemented to control the divertor neutral pressure.

The signal measured with the fast-response ionisation gauge inside the divertor plate is fed to the real-time computer [11,12], so that the command signal of the gas puffing rate, determined every 10 ms, is sent to the piezoelectric gas valve. The hydrogen or deuterium gas flow into the divertor region is changed in 100 ms, which is the delay of the gas feed system.

Fig. 2 shows an example of successful feedback control of the divertor neutral pressure performed by the hydrogen puffing in an OH discharge. Time traces are for measured divertor neutral pressure, reference pressure (top), gas puffing rate at the divertor (second), averaged

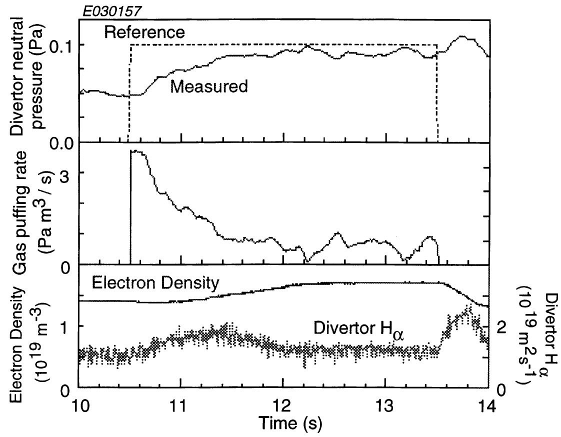

Fig. 2. Typical example of the feedback control of the divertor neutral pressure. Shown are the reference and observed divertor neutral pressure (top), gas-puffing rate (second), averaged electron density and the divertor H_α emission (bottom).

electron density and H_α emission through the inside divertor chord (third). The divertor neutral pressure is preprogrammed to stay at 0.1 Pa with a flat top duration of 3 s. A sudden increase of gas puff at around 10.5 s indicates that the gas injection is performed so as to compensate the difference between the measured pressure and the reference pressure. The gas puff becomes small as the measured pressure grows to the reference pressure. Thus, the divertor neutral pressure is successfully controlled at the reference value for about 2 s. The averaged electron density gradually increases during the feedback control of the divertor neutral pressure. Since the gas feed from the main puff is shut off during this phase, the increase of the density is due to the divertor puff.

4. Simultaneous feedback control by dual gas puff locations

The divertor neutral pressure and the main plasma density show different responses depending on the gas puff location. In Fig. 3 the averaged density along the plasma centre chord is plotted against the neutral pressure at the inside divertor for two different gas puff locations. This plot indicates different traces for different gas puff locations, that is, the main puff contributes mainly to the density increase and divertor puff contributes mainly to the divertor neutral pressure. Therefore, the simultaneous control of averaged density and divertor neutral pressure by dual feedback loop with two puffs is feasible. Fig. 4 illustrates the feedback loops of the simultaneous control. One feedback loop controls the integrated electron density along the chord near the plasma centre by main gas puff, and the other loop controls the divertor neutral pressure by divertor gas puff.

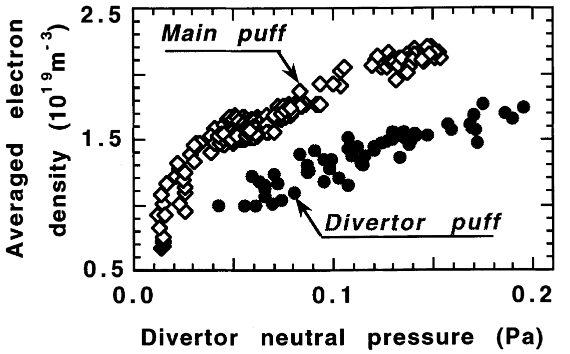

Fig. 3. Dependence of neutral pressure and average density on the gas puff location in the OH-phase of $I_p = 1.7$ MA, $B_t = 3.5$ T and X-point height of 8 cm. Diamonds and circles indicate the gas puff from the main, and from the divertor, respectively.

Fig. 5 shows the time traces of the divertor neutral pressure and averaged density, with simultaneous feedback control performed in L-mode plasma with divertor pumping. Since the averaged density is controlled in the actual feedback loop by the integrated density along the plasma centre chord, the reference and observed waveforms of the density are represented by the integrated value. Solid lines in the boxes are reference waveforms, one of which is kept constant while the other is increased. The first example (Shot E030412) shows the time traces of a relatively well-controlled shot. Observed divertor neutral pressure and averaged density well follow the reference by each corresponding gas puff. On the contrary, in the second and the third examples the control was not successful. In the second example (Shot E030414), the reference of the divertor neutral pressure is set higher than in the first example. The averaged density exceeds the reference at the timing of the second flat top of the divertor neutral pressure. On the other hand, the divertor neutral pressure is well controlled. In the third example (Shot E030416) the reference of the averaged density is set higher than in the first example. This time, the actual divertor neutral pressure exceeds the reference at the early phase of the flat top. On the other hand, the averaged density is well controlled. During the out-of-control phase in the second and the third examples, gas is not injected from the corresponding gas valve. The increase of the out-of-control parameter is due to increase of the cross-term coupling of divertor neutral pressure with the main gas puff and of the main density with the divertor gas puff, so that the feedback control loop cannot be properly operated. This tendency suggests that the feasibility of the simultaneous feedback control is limited at a moderate range of divertor neutral pressure and averaged density.

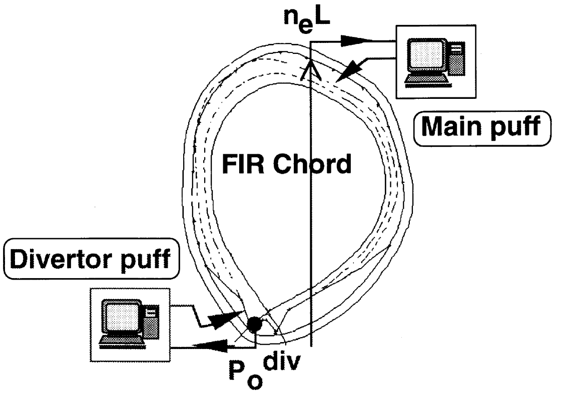

Fig. 4. Feedback loops of the simultaneous control of integrated electron density, n_{eL}, and of divertor neutral pressure, P_0^{div}.

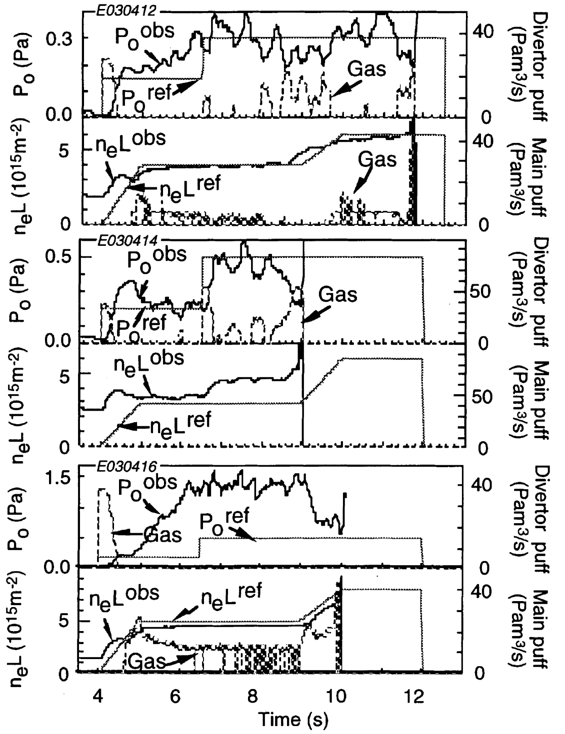

Fig. 5. Temporal behaviours of the divertor neutral pressure, P_0 the line integrated density along the centre chord, n_{eL}, and the corresponding gas puff during simultaneous feedback control for three different shots. Superscripts obs and ref indicate the observed and reference traces, respectively.

5. Contributions of each gas puff

From typical examples of simultaneous feedback control, existence of the relatively strong coupling of each gas puff with averaged density and neutral pressure has been found out. Therefore the coupling is assumed to be described as

$$\begin{pmatrix} n_e \\ P_0 \end{pmatrix} = \begin{bmatrix} f_{nM} f_{nD} \\ f_{pM} f_{pD} \end{bmatrix} \begin{pmatrix} V_M \\ V_D \end{pmatrix}, \tag{1}$$

where f_{nI}, f_{pI}, and V_I are coupling coefficients of averaged density with gas puff, that of neutral pressure and the gas puff rate, while the suffix I denotes the gas puff into the main ($I = \mathrm{M}$) and into divertor ($I = \mathrm{D}$). Coupling coefficients are the functions of divertor geometry and of plasma parameters.

Each coupling coefficient is estimated from the response to the single gas puff of pre-programmed pulse. For each response to single gas puff of V_I, Eq. (1) is rewritten as

$$\begin{pmatrix} f_{nI} \\ f_{pI} \end{pmatrix} = \begin{pmatrix} n_e \\ P_0 \end{pmatrix} \frac{1}{V_I} \quad (I = \mathrm{M}, \mathrm{D}). \tag{2}$$

In the ohmic discharge of $I_p = 1.7$ MA, $B_t = 3.5$ T, with relatively low X-point height of 8 cm and without divertor pumping, the coupling coefficients are deduced:

$$\begin{bmatrix} f_{nM} = 5.7 \times 10^{18} f_{nD} = 0.81 \times 10^{18} \\ f_{pM} = 0.65 \times 10^{-2} f_{pD} = 1.0 \times 10^{-2} \end{bmatrix}. \tag{3}$$

In this case the ratio of coupling $f_{nD}/f_{nM} = 0.14$ and $f_{pM}/f_{pD} = 0.65$, indicates more contribution from main gas puff to divertor pressure than that from divertor gas puff to averaged density. Fig. 6 shows the parameter plots of simultaneous feedback control in the ohmic discharge with the same configuration as above. The cases of single gas puff alone are also indicated by two lines (for $V_M = 0$ and $V_D = 0$). Increase rate of the averaged density changes at around 1.5×10^{19} m^{-3}, the reason is not well understood but might be considered as a neutral shielding by the plasma. Due to this change of the rate, not all the regions between two border lines of $V_M = 0$, and $V_D = 0$ are feasible, and the divertor neutral pressure is easily increased.

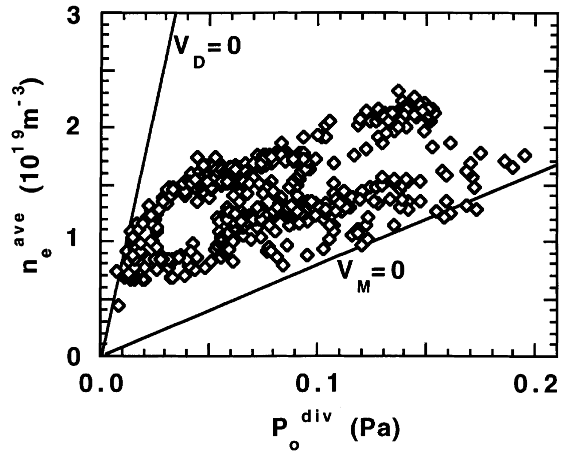

Fig. 6. Parameter plots of simultaneous feedback control in the ohmic discharge. The cases of single gas puff are indicated by two lines (for $V_M = 0$, and $V_D = 0$).

6. Discussion

Change of the coupling coefficients is expected in a different divertor geometry or in a different heating phase. Coupling coefficients are compared at the higher X-point height (16 cm) in the same ohmic discharge of $I_p = 1.7$ MA, $B_t = 3.5$ T. With a gas puff only into the divertor region ($V_M = 0$), the coupling coefficient for the divertor neutral pressure, f_{pD}, decreases to 0.007, which is about 30% as small as that at the lower X-point height of 8 cm. However, the coupling coefficient for the averaged density, f_{nD}, increases to 1.5×10^{18}, which is about 85% as large as that at the X-point height of 8 cm. These trends suggest that the lower X-point height is effective for isolation of the main plasma from divertor neutral particles. By lowering the X-point height, the X-point becomes closer to the private dome and the inner hit point becomes closer to the pumping duct. It is not clear yet which is dominantly effective for the isolation of main plasma from the divertor neutral particles.

Fig. 7 shows the change in the divertor neutral pressure (P_0^{div}, indicated by the circles) and in the averaged density (n_e^{ave}, indicated by diamonds) during the sweep of the X-point height in a single shot (E030947) at the different

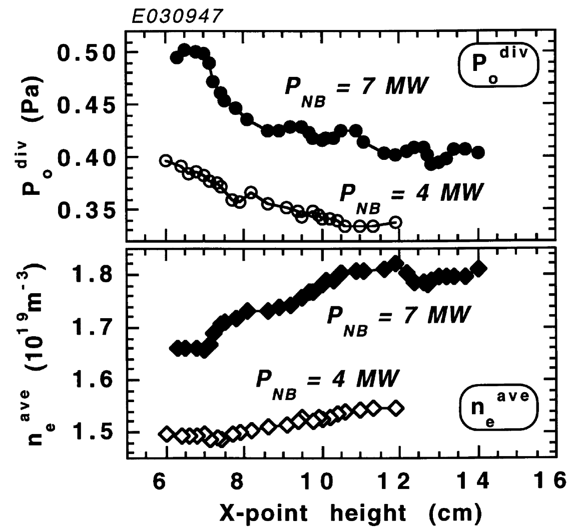

Fig. 7. Change in divertor neutral pressure (P_0^{div}, indicated by circles) and in averaged density (n_e^{ave} , indicated by diamonds) during the sweep of the X-point height in a single shot (E030947) at two NB heating powers (P_{NB}). Solid and open marks denote the NB power of 7 and 4 MW, respectively.

ferent NB heating power (PNB). Solid and open marks denote the NB power of 7 and 4 MW, respectively. At the first sweep of X-point height from 6 to 14 cm NB power is kept at 7 MW. Consequently, at the second returning sweep from 14 to 6 cm NB power is kept at 4 MW. In both sweeps by lowering the X-point height, the divertor neutral pressure increases and the averaged density decreases, therefore, the same dependence on X-point height in the NB heating phase as that in the ohmic phase is confirmed. Moreover, there seems to exist the power dependence. The divertor neutral pressure and the averaged density in the first sweep at 7 MW of NB power are much larger than those in the second step at 4 MW. The power dependence comes from the differences in particle source and in particle confinement. In the NB heating phase, no gas is fed from the gas puffs into the main plasma and the divertor. NB is the only particle source. Therefore, in high NB power region, the controllability by gas puff is expected to be very much limited.

Fig. 8 shows the changes of the divertor neutral pressure and the averaged density in the OH, in L-mode, and in the ELMy H-mode, in the discharge of $I_p = 1.7$ MA, $B_t = 3.5$ T, with X-point height of 8 cm. Triangles and circles denote the gas puff into the main plasma and the gas puff into the divertor, respectively. In the ELMy H-mode, the parameter window for the divertor neutral pressure and the averaged density extends to the high flux region. However, the width of the parameters becomes narrower and the difference of the gas puff location becomes small. Ratio of coupling coefficients for the single gas puff, defined as f_{nI}/f_{pI} ($I =$ M, D), is compared in the OH, L-mode and ELMy H-mode, as shown in Table 1. Ratio indicates the degree of the coupling of averaged density with gas puff, compared to that of divertor neutral pressure with gas puff. Both the ratios for main and divertor gas puff decrease by turn, in the OH, L-mode and in the ELMy H-mode. Therefore in the high recycling region, divertor pressure is easily increased, but the averaged density saturates. In order to improve the fuelling efficiency to the main plasma, for example, pellet injection must be made.

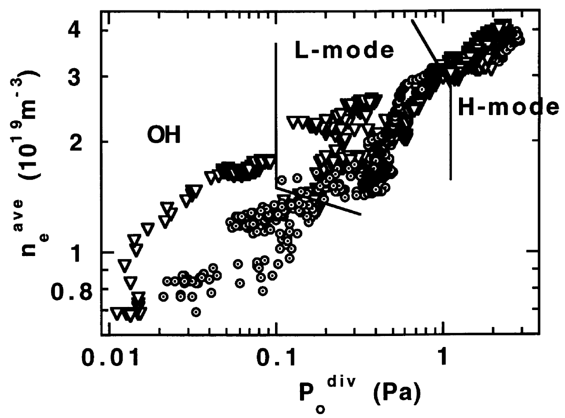

Fig. 8. Changes in divertor neutral pressure and averaged density in OH, in L-mode ($P_{NB} = 4$–10 MW), and in ELMy H-mode ($P_{NB} = 20$ MW), in the discharge of $I_p = 1.7$ MA, $B_t = 3.5$ T, with X-point height of 8 cm. Triangles and circles denote the gas puff into the main plasma, and that into the divertor, respectively.

Table 1
Comparison of the ratio of coupling coefficients

	$f_{nM}/f_{pM}(V_D = 0)$	$f_{nD}/f_{pD}(V_M = 0)$
OH	8.5×10^{19}	4.2×10^{19}
L-mode	3.8×10^{19}	1.7×10^{19}
ELMy H-mode	0.73×10^{19}	0.29×10^{19}

7. Conclusions

In order to estimate the feasibility of the particle fuelling in the W-shaped divertor, which is similar to the vertical target of the ITER divertor design, a simultaneous feedback control for the divertor neutral pressure and the averaged electron density by the dual locations of gas puff is investigated. Strong cross-term coupling of the divertor neutral pressure with main gas puff limits the controllable parameter regimes for proper feedback control. Lowering the X-point height is effective for isolation of the main plasma from divertor neutral particles. During the NB heating phase, the particle flux from the beams dominates the particle flux given by the gas puff, and the difference between the main and divertor gas puff becomes small. Especially in the ELMy H-mode, the increase in the divertor neutral pressure becomes quite large.

References

[1] ITER Detail Design Report, November 1996.
[2] T. Taylor, Plasma Phys. Controlled Fusion 39 (1997) B47.
[3] O. Gruber et al., Plasma Phys. Controlled Fusion 39 (1997) B19.
[4] B. Unterberg et al., Plasma Phys. Controlled Fusion 39 (1997) B189.
[5] N. Hosogane et al., Plasma Physics and Controlled Nuclear Fusion Research, Proc. 16th Int. Conf. Montreal, 1996, vol. 3, IAEA Vienna, 1997, p. 555.
[6] N. Hosogane et al., these Proceedings.
[7] N. Asakura et al., these Proceedings.
[8] G. Haas et al., J. Nucl. Mater. 121 (1984) 151.
[9] C.C. Klepper et al., J. Vac. Sci. Technol. A. 11 (2) (1993) 446.
[10] A. Kallenbach et al., Nucl. Fusion 35 (1995) 1231.
[11] K. Kurihara et al., Nucl. Eng. Des./Fus. 11 (1990) 441.
[12] S. Konoshima et al., JAERI-Research, 96-018, 1996.